In conclusion we may remark that the contributions lying at the base of the above method of determining the effective local field in LC by experiment is evidently easier to justify by using impurity spectroscopy of the LC, because in this case the local field acting on a molecule of impurity is created mainly by molecules of the matrix, in which there is no transition to the given resonance frequency.

The author thanks L. M. Blinov and E. M. Aver'yanov for discussing the problem of the local field in liquid crystals.

[1)] Below we give references only to the latest publications.

[2)] Exchange of the molecule by a dielectric ellipsoid[13,15,6] in the microscopic theory is equivalent to a model of point polarizability, since in an external field such an ellipsoid has the same dipole moment as a point with effective polarizability tensor.

[1]P. Mazur, Adv. Chem. Phys. 1, 209 (1958).
[2]W. De Jeu, Physical Properties of Liquid-Crystalline Substances [in Russian], Mir, Moscow (1982).
[3]M. Born and Kun Huang, Dynamical Theory of Crystal Lattices [Russian translation], IL, Moscow (1958).
[4]V. M. Agranovich, Usp. Fiz. Nauk 112, 143 (1974) [Sov. Phys. Usp. 17, 103 (1974)].
[5]D. A. Dunmur and S. W. Munn, Chem. Phys. 76, 249 (1983).
[6]Sen Sushmita, P. Brachma, S. K. Roy, and S. B. Roy, Acta Phys. Polon. A 65, 47 (1984).
[7]I. Penchev, I. Dozov, and N. J. Kirov, J. Molec. Liquids, 29, 147 (1984).
[8]E. M. Aver'yanov, V. A. Zhuikov, V. Ya. Zyryanov, and V. F. Shabanov, Zh. Eksp. Teor. Fiz. 87, 1686 (1984) [Sov. Phys. JETP 60, 968 (1984)].
[9]E. M. Aver'yanov, P. V. Adomenas, V. A. Zhuikov, et al., Zh. Eksp. Teor. Fiz. 87, 1686 (1984).
[10]L. M. Blinov, V. A. Kizel', V. G. Rumyantsev, and V. V. Titov, Kristallografiya 20, 1245 (1975) [Sov. Phys. Crystallogr. 20, 750 (1975)].
[11]L. G. P. Dalmolen, E. Egberts, and W. H. de Jeu, J. Phys. (Paris) 45, 129 (1984).
[12]S. D. Durbin and Y. R. Shen, Phys. Rev. A 30, 1419 (1984).
[13]W. H. de Jeu and P. Bordewijk, J. Chem. Phys., 68, 109 (1978).
[14]M. F. Vuks, Opt. Spektrosk. 20, 644 (1966).
[15]A. Hauger, G. Pelsl, C. Selbman, et al., Molec. Cryst. Liq. Cryst. 91, 9 (1983).
[16]U. Segre, Molec. Cryst. Liq. Cryst. 90, 239 (1983).
[17]H. S. Subramhanyan and D. Krishnamurti, Molec. Cryst. Liq. Cryst. 22, 239 (1973).
[18]M. A. Osipov, Fiz. Tverd. Tela (Leningrad) 27, 1651 (1985) [Sov. Phys. Solid State 27, 993 (1985)].
[19]M. A. Osipov, Chem. Phys. Lett. 113, 471 (1985).
[20]P. V. Elyutin, L. V. Keldysh, and A. G. Kechek, Opt. Spektrosk. 57, 282 (1984) [Opt. Spektrosc. (USSR) 57, 170 (1984)].
[21]E. M. Aver'yanov, Fiz. Tverd. Tela (Leningrad) 22, 1867 (1980) [Sov. Phys. Solid State 22, 1088 (1980)].

Translated by S. G. Kirsch

Dynamic diffraction of a spherical x-ray wave in two perfect crystals with slightly disturbed orientation

V. V. Aristov, V. G. Kon, and A. A. Snigirev

I. V. Kurchatov Institute of Atomic Energy

(Submited June 14, 1985)

Kristallografiya **31**, 1059–1065 (November–December 1986)

The authors investigate the topographical image in a scheme of dynamic diffraction of divergent x rays on two perfect crystals with slightly disturbed orientation. They give a detailed analysis of the changes in the type of interference bands of the anomalous pendellösung effect and focusing of the radiation relative to a thick crystal (150 μm) with the standard source–film distance of 40 cm. It is shown that with a sufficiently large angle of disorientation the diffraction pattern is two images of the first crystal, separated by the second crystal only with slight distortion. All the features of the experimental topograms are in full agreement with the theory of diffraction of spherical waves in two crystals. The experiment is numerically modeled on a computer.

1. INTRODUCTION

In Refs. 1–8 it was shown that the possibilities of standard sectional topography can be broadened if we register the diffraction pattern at a distance from the radiation source. In conditions with diffraction of a spherical wave by a perfect crystal with a definite value of t/L, where t is the thickness of the crystal, L is the source–film distance, a new physical phenomenon arises – focusing of x-radiation in a vacuum.[1–4] The essence of this phenomenon is that the changes in the wave front moving in vacuum and in the crystal are mutually compensated. Distortion of the wave front in vacuum also complicates the form of the interference pattern in schemes using diffraction by two crystals. In such a scheme the effect of sharp focusing[9] takes place even in the case L = 0 with satisfaction of the condition $t_1 = t_2$, where t_1 and t_2 are the thickness of the first and second crystals, respectively. In Refs. 6–8 the scheme of diffraction by two crystals was analyzed in the more general case $L \neq 0$. With ideal adjustment of the crystals, three of the four wave fields arising in these conditions are focused with various relations between t_1, t_2 and L. Experimentally it is easy to realize the case of ideal adjustment if both crystals are cut from one block of a perfect single crystal.[9–10] With two crystals in general a new possibility arises for investigation in conditions of nonideal adjustment of the crystals. On experimental topograms there then arises a complex pattern requiring careful analysis. In the case of weak disorientation of the crystals this problem was analyzed in Refs. 8, 10.

This article is devoted to theoretical and experimen-

 0038-5636/06/66 0626-05 $03.90

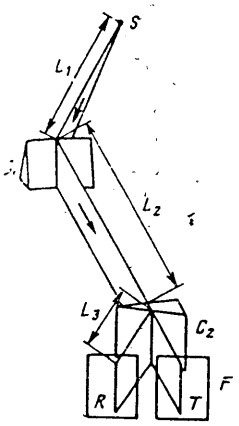

FIG. 1. Scheme of experiment. S) Source; C_1) first crystal; C_2) second crystal; F) photographic film.

tal investigation of the diffraction of a spherical wave in the general case of arbitrary disorientation and arbitrary ratios between t_1, t_2, and L. In Sec. 2 we describe the experimental scheme and give experimental topograms. In Sec. 3 we give a theoretical interpretation of the results on a basis of model calculations made in the framework of the theory developed in Ref. 6. The theoretical topograms excellently reproduce all the details of the experimental topograms, in particular the bands of the anomalous pendellösung effect.[4]

2. EXPERIMENTAL

The scheme of the experiment is shown in Fig. 1. Radiation from a Microflex microfocus x-ray generator made by the firm Rigaku Denki with a focus measuring not more than 10 μm falls directly on the first crystal, cut in the form of a wedge with the wedge angle in a plane perpendicular to the scattering plane. The slit, fixed in front of the first crystal, has a width of more than 100 μm, and, in contrast with the usual sectional topography, serves only to separate the spectral line Au Lα with wavelength $\lambda = 1.276$ Å. The second crystal is also wedge-shaped, but the wedge angle is small (about 2°) and lies in the plane of scattering. Therefore in the vertical direction it is plane, and the changes in its thickness over the width of the x-ray beam can be neglected. The use of wedge-shaped crystals enables us to fairly simply investigate the diffraction of x rays in thin crystals, using the thin part of the wedge.

The parameters of the experimental scheme had the following values: $L_1 = 10$, $L_2 = 20$, $L_3 = 1$ cm. Investigations were made both on identical crystals (Ge or Si) and on different crystals (first Ge, second Si). Preliminary adjustment was made by means of the integral reflection with the aid of a counter, after which a topogram was taken.[1)] The exposure time was from a few tens of minutes to several hours. Figure 2 shows typical topograms for two identical Ge crystals using the 111 reflection. We considered beams reflected in the first crystal and transmitted (T) or reflected (R) in the second crystal 100 μm thick. Since the second crystal was plane, the difference of the diffraction patterns on the topogram is not great. In both cases the pattern is double: On the right-hand side we see the bands of the anomalous pendellösung effect,[4] corresponding to relatively long path of the rays in vacuum, and on the left-hand side on the other hand the image broadens from top to bottom as if the focus were

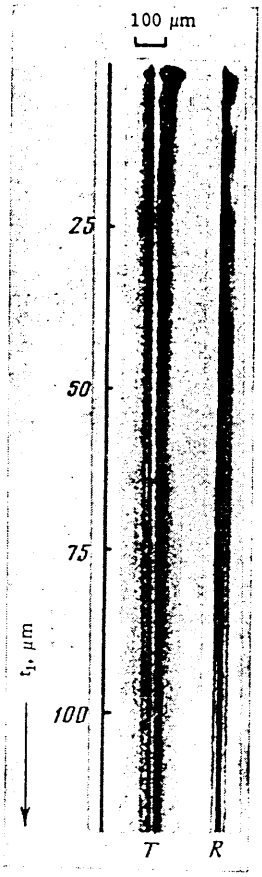

FIG. 2. Experimental topograms in the case of two disoriented crystals of germanium. $\psi_h \approx 10''$, 111 reflection radiation Al Lα ($\lambda = 1.276$ Å; R) doubly reflected beam; T) beam reflected by first crystal and transmitted by the second (cf. Fig. 1).

above. Moreover, whereas on the R topogram the two images practically coalesce, on the T topogram they are distinctly separated by a bright band. One also notes the asymmetry of the left-hand image on the R topogram. As it turned out, all these features are well described in the framework of the theory in Ref. 6, discussed in more detail in the next section.

3. THEORY

For simplicity we shall confine ourselves to the case of two identical crystals. Using the integral representation of an incident spherical wave and considering the propagation of partial plane waves in two crystals taking account of their phase changes in the vacuum, in Ref. 6 we obtained an expression for the spatial dependence of the intensity of radiation in the plane of the topogram in the form of a single integral

$$I_H(x) = \frac{\lambda d}{L} \sum_s |G^{HS}(x)|^2, \tag{1}$$

$$G^{HS}(x) = \sum_{jj'} \int_{-\infty}^{\infty} \frac{dq}{2\pi} f_{jj'}^{HS}(q) \exp(iqx + i\varphi_{jj'}^{s}(q)), \tag{2}$$

where λ is the wavelength of the radiation, 2d is the dimension of the focus of the x-ray tube, $L = L_1 + L_2 + L_3$ (see Fig. 1), the index S determines the state of polarization of the radiation (π or σ), and the indices j and j' number the zones of the dispersion surface (DS) in the first and second crystals. The phase $\varphi_{jj'}^{S}(q)$ is equal (for simplicity below we omit obvious indices) to

$$\varphi(q)=x_0 q-\frac{\lambda L}{4\pi}q^2+\frac{\sin\theta_B}{\Lambda}(z_j B_1(q)t_1+z_{j'}B_2(q)t_2), \quad (3)$$

where

$$B_n(q)=(1+y_n^2(q))^{1/2}, \quad n=1,\ 2, \quad (4)$$

and the amplitude $f_{jj'}^{SH}(q)$ takes the form

$$f(q)=R_j^{(1)}(q)A_{Hj'}^{(2)}(q)\exp\left(-\frac{1}{2}(\mu_j^{(1)}(q)t_1+\mu_{j'}^{(2)}(q)t_2)\right), \quad (5)$$

where

$$\mu_j^{(n)}(q)=\frac{\mu_0}{\cos\theta_B}\left[1-z_j\frac{|\chi_{ih}|}{\chi_{i0}}\frac{c_s}{B_n(q)}\right] \quad (6)$$

is the interference coefficient of the absorption, and

$$R_j^{(1)}(q)=-\frac{z_j}{2B_1(q)}, \quad A_{Hj'}^{(2)}(q)=\begin{cases}-\dfrac{z_{j'}}{2B_2(q)}, & H=R\\ \dfrac{1}{2}\left(1+z_{j'}\dfrac{y_2(q)}{B_2(q)}\right), & H=T\end{cases} \quad (7)$$

is the scattering amplitude of the diffracted waves, where H = R for the reflected and H = T for the transmitted beam in the second (plane) crystal.

The parameters of deviation from the Bragg condition $y_n(q)$ in each of the crystals are

$$y_1=\Lambda(q+q_0), \quad y_2=\Lambda(-q+q_0), \quad (8)$$

where the angle of disorientation of the crystals ψ_h occurs in the theory via the parameters

$$q_0=\pi\psi_h/\lambda, \quad x_0=-\frac{1}{2}L\psi_h \quad (9)$$

with the condition that $L_2 = L_1 + L_3$ (condition of polychromatic focusing). The rest of the notation is the same as in Ref. 6, e.g.,

$$\Lambda=\frac{\lambda}{2\pi}\frac{\sin 2\theta_B}{|\chi_{rh}|C_s}, \quad (10)$$

where C_s is the polarization factor, θ_B is the Bragg angle, and $\chi = \chi_r + i\chi_i$ is the polarizability of the crystal.

With values of the parameters corresponding to typical experimental conditions, the integral in (2) can be estimated with fair accuracy by the stationary phase method.[11] In contrast with Ref. 6, here we are interested in the case in which $\psi_h \neq 0$. Then

$$G_{(x)}^{HS}=\sum_q\left(\frac{i}{4\pi}\right)^{1/2}\sum_{jj'}f_{jj'}^{HS}(q)\frac{\exp(iqx+i\varphi_{jj'}^{\ s}(q))}{K_{jj'}^{\ s}(q)}. \quad (11)$$

In expression (11) the sum is taken over those values of q which satisfy the equation

$$x=-x_0+\frac{\lambda L}{2\pi}q+\sin\theta_B\left(-\frac{z_j y_1(q)}{B_1(q)}t_1+\frac{z_{j'}y_2(q)}{B_2(q)}t_2\right), \quad (12)$$

and the denominator is equal to

$$K_{jj'}^{\ s}(q)=\left(\frac{d^2\varphi_{jj'}^{\ s}(q)}{dq^2}\right)^{1/2}=\left[-\frac{\partial x}{\partial q}\right]^{1/2}$$
$$=\left[-\frac{\lambda L}{2\pi}+\sin\theta_B\Lambda\left(\frac{z_j t_1}{B_1^3(q)}+\frac{z_{j'}t_2}{B_2^3(q)}\right)\right]^{1/2}. \quad (13)$$

Equations (1)–(13) enable us to calculate the topogram for various values of the disorientation angle ψ_h.

Before the results of the numerical calculation, let us consider first the qualitatively simple case in which the angle of disorientation is sufficiently large. Then the central part of the DS of the first crystal ($y_1 \approx 0$) corresponds to the tail of the DS of the second crystal ($|y_2| \gg 1$), and conversely, when $y_2 \approx 0$, then $|y_1| \gg 1$. Let us consider the first case in which $q = -q_0 + \Delta q$ and $|\Delta q|$ is small. Expanding in a power series in terms of Δq, we obtain the approximation

$$x=z_{j'}\operatorname{sign}(\psi_h)\sin\theta_B t_2(1+(2\Lambda q_0)^{-2})^{-1/2}$$
$$+\Delta q\left[\frac{\lambda L}{2\pi}-\sin\theta_B\Lambda\left(z_j t_1+\frac{z_{j'}t_2}{B_2^3(-q_0)}\right)\right]. \quad (14)$$

According to Eq. (14) the angular region corresponding to the exact Bragg position of the first (wedge-shaped) crystal, on account of scattering in the second crystal, gives two different images, which with a large angle of disorientation ψ_h are displaced one relative to the other by a distance of order $2\sin\theta_B t_2$. The scattering in the second crystal is kinematic in character; therefore the intensity of the reflected beam is relatively low, but approximately the same in both images, while the intensity of the transmitted beam is different owing to the different amplitudes of passage corresponding to different zones of DS of the second crystal.

From (14) it is also easy to determine the thickness of the first crystal which corresponds to focusing of the radiation. For this it is necessary that the coefficient of Δq shall be zero. As before, we shall mark the wave fields by the letters A (j = 2) and B (j = 1). For the most interesting BA field we have

$$t_{1f}^{BA}=\frac{\lambda L}{2\pi\Lambda\sin\theta_B}+\frac{t_2}{\left[1+\left(2\pi\frac{\Lambda}{\lambda}\psi_h\right)^2\right]^{1/2}}=t_S+Kt_2. \quad (15)$$

The first term of this expression is equal to the depth of focusing of the first crystal necessary for compensation of the phase change of the wave moving in a vacuum.[4] The second term increases the depth of focusing, i.e., it plays in fact the same role as the vacuum, but the degree of increase depends on the angle of disorientation. Since the AA and BA fields give images in one place on the topogram their interference also leads to a large number of bands of the anomalous pendellösung effect even with a relatively short source–film distance, which can be seen in the right-hand part of the experimental topogram (Fig. 2). Thus in the experiment $\psi_h < 0$.

Focusing of the BB field occurs at a thickness $t_{1f}^{BB} = t_S - Kt_2$, but the image is on the left. It is interesting that with increase of the angle of disorientation ψ_h the thicknesses of the first crystal corresponding to focusing of the BA and BB fields converge, but the image itself spatially increasingly diverges. In a scheme with a small value of L focusing of the AB field is possible with a thickness $t_{1f}^{AB} = Kt_2 - t_S$, but in this case the focus rapidly becomes negative with rise in ψ_h.

Clear information on the contributions of various fields to the formation of the image can be obtained by a very simple means if we draw on the plane of the parameters (x, t_1), corresponding to the topogram from a wedge-shaped crystal, the lines $x(t_1)$ by means of (12) for given values of the experimental parameters L, t_2 and values of the angular parameter $\Delta q = q + q_0 = y_1/\Lambda$ at constant intervals. Figure 3 shows diagrams of this type for the case of two Ge crystals, 111 reflection, Au Lα radiation, L = 40 cm, and t_2 = 100 μm (which corresponds to the experi-

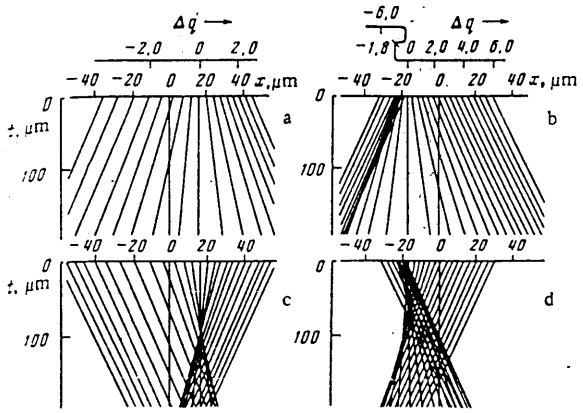

FIG. 3. Diagrams showing "angular density" of decomposition of spherical wave on topogram for wave fields of types AA (a), AB (b), BA (c), and BB (d).

mental topograms in Fig. 2). The angle of disorientation is $\psi_h = -0.05$ mrad (approximately 10 arcsec). Since the lines correspond to changes in the angular parameter at equal intervals (the value is given at the top of the diagram), convergence of the lines corresponds to optical increase in intensity, and divergence to a decrease (scattering). Therefore topograms of this type show the angular density of separation of a spherical wave in various parts of the topogram. On them we clearly see regions of focusing, caustics, superposition of two angular regions in one place, etc. They are very useful in planning an experiment, because they enable us to quickly and simply determine the main characteristics of the image for particular conditions.

To obtain the full pattern of interference of the fields it is necessary to carry out a numerical calculation on a computer by means of Eqs. (1)-(13). The results of the calculation for the stated values of the parameters are shown in Fig. 4. The calculation was made for σ-polarized radiation with the aim of elucidating the maximally sharp pattern of interference bands. Comparison of Figs. 2 and 4 shows that the main features of the experimental topograms are excellently reproduced in the calculated ones. Note the difference of the T and R topograms for large values of t_1. The central black band on the R topogram corresponds to a brighter asymmetric band on the T topogram.

This band is formed mainly by the BB field; its left-hand side corresponds to large positive values of Δq (see Fig. 3). In this region $y_2 < 0$ and $|y_2| \gg 1$. Therefore, according to (7), for the BB field the transmitted amplitude in the second crystal is much less than the reflected amplitude. In general the central part of the T topogram corresponds to fields which are "forbidden" in the kinematic approximation in the sense that the direction of the current of energy in the second crystal for these zones differs by $2\theta_B$ from the direction of the incident beam. Conversely, the edge of the T topogram is well transferred by the second crystal in practically a diffraction-free regime.[2)]

In sum we can draw the conclusion that the scheme of experiment with two slightly disoriented crystals, while preserving all the advantages of a scheme with one crystal,[4] i.e., focusing and an anomalous type of interference

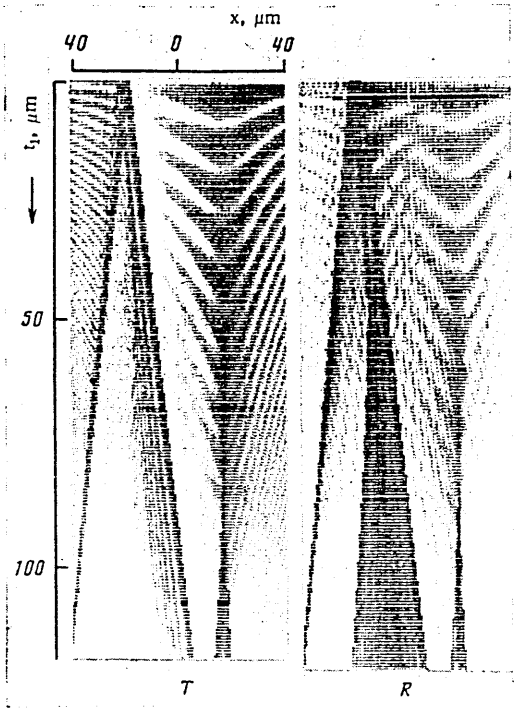

FIG. 4. Calculated topograms for case corresponding to Fig. 2.

bands, is in some cases more convenient for investigating the defect structure of the first crystal, because there appears the additional possibility of controlling the parameters of the experimental scheme, for example, changing the depth of focus of the first crystal by changing the angle of disorientation.

Note also that in some cases focusing of the radiation on the photographic plate is accompanied by focusing of the radiation in the crystals. This follows from the equation first derived in Ref. 1, linking the thickness t of the crystal to the source-film distance L. If instead of L, in this expression we put L_1, the source–crystal distance, then we obtain the depth of the crystal $z = tL_1/L < t$ at which is focused the radiation in the crystal. In Ref. 1 this property of the focusing was not discussed, and in Ref. 12 it was obtained independently by a different method. In our case the depth of the crystal at which the radiation is focused can also be obtained from Eq. (14). Thus for the BA field, replacing L by L_1 and putting $t_2 = 0$, we obtain the depth $z = t_S L_1/L < t_S$ of focusing of the BA field in the first crystal.

According to (15), focusing in the second crystal takes place if $z = (t_1 - t_S)/K < t_2$. We must also remember that in the case of polychromatic radiation this focusing is not actually realized, since the points of focusing for different frequencies are "blurred" over the crystal. They can be observed only with monochromatic radiation.[13] When the characteristic radiation of x-ray tubes is used, the focusing can actually be observed only in vacuum with satisfaction of the condition of polychromatic focusing simultaneously with the condition of diffraction focusing.

The above results also show the effectiveness of the scheme of calculation described above for numerical modeling of experiment. This scheme can be used also in more complex situations of slowly changing fields of deformation in the crystal.

[1)]In the experiment the disorientation was first established by tilting the second crystal from the exact Bragg position, the reading being taken from the dial of the goniometer (scale division 1"). The accuracy of this setting was verified from the splitting of the images on the topograms.

[2)]Note that in the case of different crystals the pattern should not differ in principles from that for identical crystals, but nonmonochromaticity of the radiation does not allow us to observe the fine structure of the image in the proposed experimental scheme if the Bragg angles of the first and second crystals differ widely.[6]

[1]A. M. Afanas'ev and V. G. Kon, Fiz. Tverd. Tela (Leningrad) 19, 1775 (1977) [Sov. Phys. Solid State 19, 1035 (1977)].

[2]V. V. Aristov, V. I. Polovinkina, et al., Pis'ma Zh. Eksp. Teor. Fiz. 28, 6 (1978) [JETP Lett. 28, 4 (1978)]

[3]V. D. Koz'mik and I. P. Mikhailyuk, Ukr. Fiz. Zh. 23, 1570 (1978).

[4]V. V. Aristov, V. I. Polovinkina, A. M. Afanas'ev, et al., Acta Cryst. A 36, 1002 (1980).

[5]V. V. Aristov, V. G. Kohn, V. I. Polovinkina, et al., Phys. Status Solidi a 72, 483 (1982).

[6]V. V. Aristov, A. A. Snigirev, A. M. Afanes'ev, et al., Acta Cryst. A 42, (1986) (in press).

[7]V. V. Aristov, W. Graeff, V. I. Polovinkina, and A. A. Snigirev, Prepr. DESY, Hamburg (1984), Phys. Status Solidi a 90, 69 (1985).

[8]L. V. Levonyan, Intercollegiate Symposium of Scientific Work [in Russian], Fizika, Erevan (1984), No. 3, 42.

[9]V. L. Indenbom, I. Sh. Slobodetskii, and K. G. Truni, Zh. Eksp. Teor. Fiz. 66, 1110 (1974) [Sov. Phys. JETP 39, 542 (1974)].

[10]V. L. Indenbom, É. V. Suvorov, and I. Sh. Slobodetskii, Zh. Eksp. Teor. Fiz. 71, 359 (1976) [Sov. Phys. JETP 44, 187 (1976)].

[11]G. Jefferies and B. Swirls, Methods of Mathematical Physics [Russian translation], Vol. 3, Mir, Moscow (1970).

[12]L. V. Levonyan, Pis'ma Zh. Tekh. Fiz. 7, 269 (1981) [Sov. Tech. Phys. Lett. 7, 116 (1981)].

[13]V. V. Aristov, I. Ichikawa, S. Kikuta, et al., Jpn. J. Appl. Phys. 20, 1947 (1981).

Translated by S. G. Kirsch

Three-crystal x-ray spectra of crystals with disturbed surface layer in slipping Bragg–Laue geometry

A. M. Afanas'ev, P. A. Aleksandrov, A. A. Zav'yalova, R. M. Imamov, and A. A. Lomov

Institute of Crystallography, Academy of Sciences of the USSR

(Submitted August 26, 1985)

Kristallografiya **31**, 1066–1069 (November–December 1986)

The authors investigate the possibilities of three-crystal x-ray diffractometry in slipping Bragg–Laue geometry for analysis of the structural perfection of the boundaries. From the example of a single crystal of Si implanted with B^+, they demonstrate the high sensitivity of the method in the study of disturbed layers 10–1 nm thick.

Three-crystal x-ray diffractometry (TXD) is an informative nondestructive method of investigating the real structures of crystals. The method is based on an analysis of the angular distribution of the intensity of x-rays reflected by the test crystal, as a result of which there appears the possibility of separate measurement of the intensity of dynamic and diffuse components of the full scattering.[1–4]

The dynamic component is related to the pure Bragg reflection from the specimen, but the diffuse component is due mainly to scattering by fields of displacements of lattice defects. Investigation of each of the components of full scattering gives its own information on the crystal. At present there is a very urgent problem of investigating the structures of the surface and transition layers of highly perfect, practically defect-free crystals before and after various technological procedures. Investigations of this kind are possible in the study of the dynamic component of radiation reflected from the crystal.[5–7]

Recently[8–10] there has been realized a three-crystal scheme of diffraction of x rays in slipping Bragg–Laue geometry. The test crystal has a small bevel angle $\varphi \approx 4°$, and diffractive scattering in it occurs from crystallographic planes almost perpendicular to the entry surface. The radiation reflected from the crystal is analyzed, as in the usual scheme, with the aid of a third crystal, which makes it possible to measure with good angular resolution the distribution of the intensity of rays diffracted from the test crystal. In the slipping Bragg–Laue geometry one can effect angular scanning both with respect to the Bragg angle $\Delta\theta$ ("parallel" scanning)[6,8] and with respect to the angle of emergence of the diffracted rays Φ_h ("perpendicular" scanning). In the latter case the analyzer crystal can be replaced by a scanning detector with a slit.[10]

As in the usual scheme of TXD, in slipping Bragg–Laue geometry in general we observe three peaks in the spectra: principal, pseudo, and diffuse. In Refs. 8–10 there were established the main laws of formation of peaks in the case of ideal crystals – the principal and pseudo. Thus the intensity of the principal peak is given by the following simple expression:

$$I_{rn}(\Delta\theta) = \frac{\chi_h^2}{4\Phi_0\Phi_h}\frac{1}{\delta^2}, \tag{1}$$

where χ_h is a Fourier component of the polarizability tensor, Φ_0 is the glancing angle of incidence of the x rays on the crystal

$$\Phi_h = \sqrt{\Phi_h^{02} - \alpha}, \tag{2}$$

$$\Phi_h^0 = \Phi_{h(\alpha=0)} = \Phi_0 - \psi, \tag{3}$$

$$\alpha = -2\sin 2\theta_B \Delta\theta, \tag{4}$$

$$\delta = \Phi_h - \Phi_h^0, \tag{5}$$

0038-5638/06/86 0630-03 $03.90